Structures at the electrodes of gas discharges

K. G. Müller
Institut für Laser- und Plasmaphysik, Universität Essen, Universitätsstrasse 5, D-4300 Essen, Federal Republic of Germany
(Received 5 November 1987)

A phenomenological model is developed to explain single spots or regular patterns of spots at the electrode of gas discharges. The electrodic discharge parts are described by bistable layers, governed by a time-dependent Ginsburg-Landau equation or reaction-diffusion equation; the space between the electrodic layers is taken into account by a resistive region. The steady state of a bistable layer is characterized by an *S*-shaped voltage-current density characteristic. If one bistable layer dominates the interelectrodic space, one single spot may occur. A resistive region may help to stabilize a system of spots and causes a Coulombic interaction of the spots. From a Lyapunov function, equations of motion of the spots can be derived. An initial system of spots relaxes to a stable or metastable state. Experimentally found patterns of anode spots in a glow discharge can be reproduced.

I. INTRODUCTION

During the last few decades structures as a result of self-organization have fascinated scientists of various disciplines (see, e.g., Nicolis and Prigogine,[1] Haken,[2] and Ebeling and Ulbricht[3]). However, in the field of gas discharges, which are well known by their colorful phenomena, a variety of structures still are to be explained. This investigation is focused on plasma structures at the electrodes of gas discharges.

At the anode of a glow discharge on a background of a faint anode glow, a regular pattern of bright anode spots occurs (Thomas and Duffendack,[4] Rubens and Henderson,[5] and the left part of Fig. 1). These patterns show a strong resemblance to vortex patterns in rotating superfluid ^{4}He (Packard[6]). Regular patterns of cathodic spots have been detected in an arc discharge (Kesaev[7]) and in a pulsed beam-driven discharge (Nechaev *et al*[8]). A structured glow discharge can be found between a metallic and a semiconducting electrode (Radehaus, Dirksmeyer, Willebrand, and Purwins[9]).

The structures mentioned above can be characterized by a transport of electric current to an electrode concentrated in one or several spots. In the case of the anode spots with increasing current, the transport undergoes a succession of transitions from a homogeneous state to a highly structured one. The following basic effects connected with the formation of structures can be isolated (Müller[10]).

(1) Existence of two phases of low (or vanishing) and high current density.

(2) Separation of the phases, spot formation.

(3) Formation of several spots.

(4) Ordering of the spots, pattern formation.

In this paper a simple phenomenological model is developed explaining these basic effects. A bistable layer in front of an electrode will be shown to be responsible for spot formation. The bistability is introduced by an *S*-shaped voltage-current density characteristic $U_r(j)$ of the layer (see Fig. 2). For the current density j a nonlinear partial differential equation is derived, known as the time-dependent Ginsburg-Landau equation or as the reaction-diffusion equation. The one-dimensional analogue of this equation has been applied by Ross and Litster[11] and Landauer[12] to describe the ballast resistor possessing a range of constant current in its characteristic. With the help of this equation the existence of one spot can be explained. Several spots and patterns occur if the spots at the electrode are embedded into a resistive medium contacting the layer. To describe a structured glow discharge Radehaus *et al.*[9] derived a model, leading to a system of two coupled reaction-diffusion equations.

In our model the current transport through a discharge is governed by a variational principle into which a generalized potential F with a dimension of a power or an energy dissipation enters. The resistive medium contributes to F a repulsive interaction term of the spots. Stochastic elements are neglected. Patterns of spots as metastable or stable states can be constructed and compared with the patterns of anode spots found experimentally. This approach to structures is analogous to that of Campbell and Ziff,[13] who calculated distributions of vortices in superfluid ^{4}He.

II. BISTABLE ELECTRODIC LAYER, EXISTENCE OF A SPOT

A. Model zones

As a basis of a phenomenological model an electric discharge is described by model zones (see Fig. 3). The total volume between the electrodes is divided into three zones: an electrodic layer in front of each electrode and a resistive region representing the bulk of the discharge. A layer includes the sheath and the electrodic plasma, and mediates the current transition between the bulk and the electrode. For a glow discharge this description by model zones is illustrated by Table I. Analogously, the model zones of an arc discharge can be defined. The discharge parts described by an electrodic layer show the typical *S*-shaped voltage-current characteristic of a bistable resistor, Fig. 2, with a low and a high current mode (see Table II).

In this paper structures in one layer are investigated.

The other layer is taken into account by a contribution to the external resistor R_E. According to our model the interelectrodic space is built up by one thin layer adjacent to the cathode or anode, and a resistive region. Both zones contribute to the discharge voltage

$$U_D = U_L(\mathbf{r}_L) + U_{RR}(\mathbf{r}_L) \ . \tag{1}$$

$\mathbf{r}_L$ gives a position in the negligible thin layer. An external circuit, consisting of a battery or power supply of voltage U_B and of a series resistor R_E, couples the total current I through the discharge and the discharge voltage U_D.

$$U_D = U_B - R_E I \ . \tag{2}$$

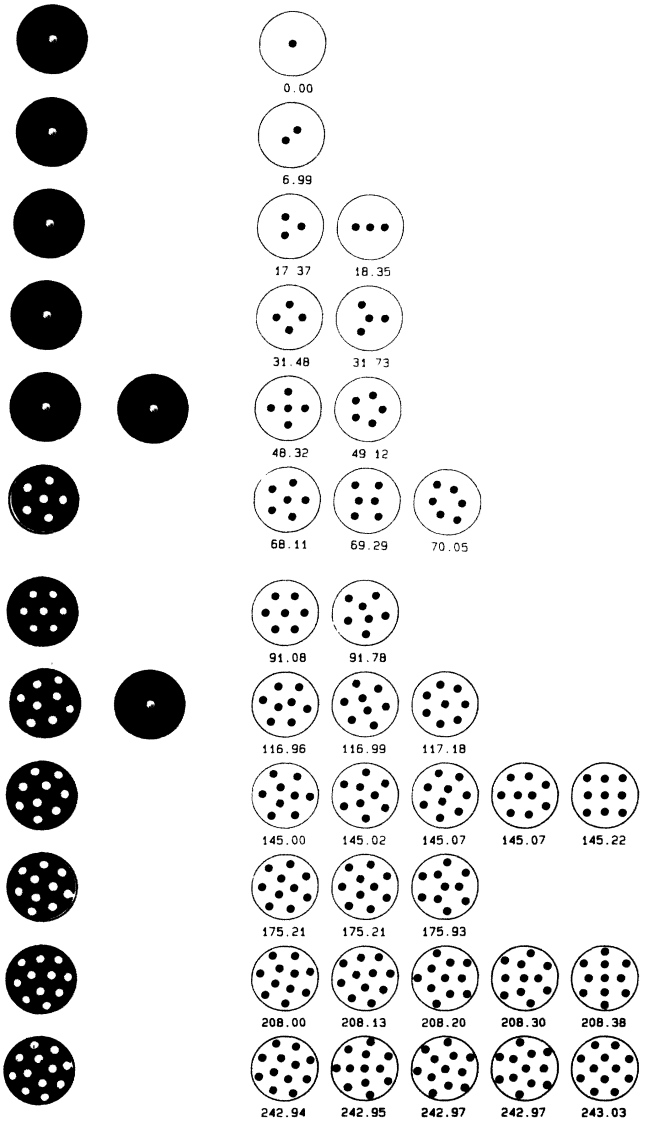

FIG. 1. Observed (left) and calculated patterns of spots at a hemispherical anode (see Sec. IV A); experimental discharge current: $(200+20N)$ mA; N: number of spots. The numbers give the value of the potential function F^*_{RR} of Eq. (68); $C_1=2$; $C_2=6$; $n=1.5$.

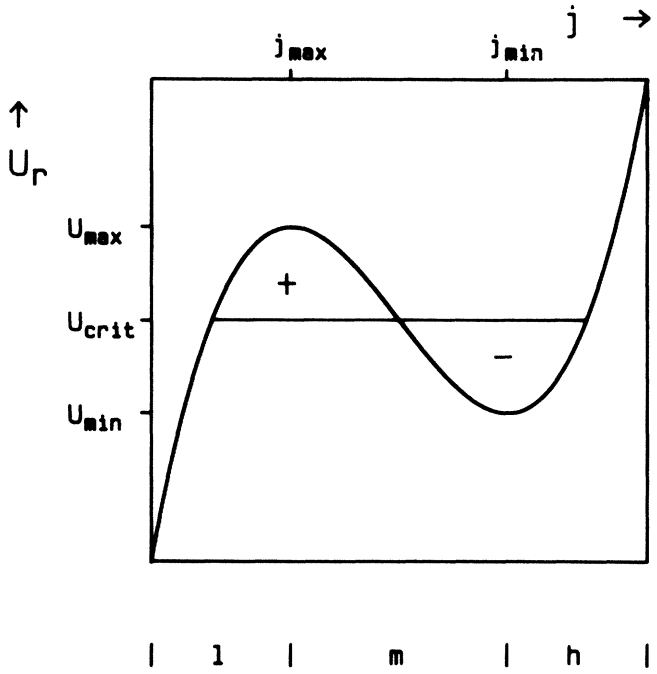

FIG. 2. Representative bistable, S-shaped voltage-current density characteristic $U_r(j)$. At the voltage $U_r = U_{crit}$ the areas + and − are equal: Maxwell's construction (see Sec. II D). l,m,h: existence regions of the low, medium, and high current modes. The subscript r indicates "resistive;" the expression S-shaped was introduced for a plot with U as abcissa and I as ordinate.

As a first step, in this section a reduced model is used, where the interelectrodic space is dominated by one layer,

$$U_{RR}(\mathbf{r}_L) = 0 \ . \tag{3}$$

The layer voltage U_D becomes spatially constant.

B. Layer model

A thin layer in front of an electrode is investigated; the radius of curvature of the electrode is assumed to be large compared to the radii of the spots discussed in the following. The current transport through the layer is governed

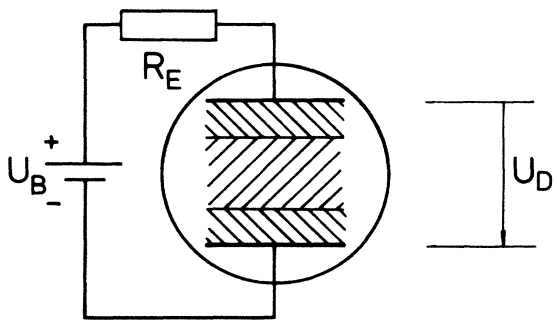

FIG. 3. Gas discharge, described by modes zones, in a simple external circuit; —— : electrode, ▨ layer, ▨ : resistive medium.

TABLE I. Model zones and discharge parts of a glow discharge.

Cathodic layer	Cathode fall region, negative glow
Resistive region	Faraday's dark space, positive column
Anodic layer	Anode fall region with anode glow, anode spots

by a voltage balance describing how different effects contribute to the total voltage U_L across the layer. A homogeneous steady layer only shows the resistive voltage drop $U_r(j)$ with an S-shaped characteristic of the type of Fig. 2. For the representative example of the cathodic parts of the glow discharge one may try to explain the bistable $U_r(j)$ characteristic. The maximum close to $j=0$ corresponds to the breakdown voltage. The basic mechanisms in the cathode fall region determining the $U_r(j)$ characteristic of the ignited glow discharge are electron multiplication, ion motion in the field of their space charge, electron emission of the cathode due to incoming ions, and ion flow from the negative glow (see, e.g., Ward[16]). According to the measurements of Melekhin and Naumov[17] the minimum of the $U_r(j)$ characteristic is correlated with the maximum of electron multiplication.

Relaxation effects of the layer can be included in the description by assigning an inductance l to an unit area of the layer; a simple model arises, allowing stability analysis of homogeneous layers. However, the spatial distribution of the current density still is indefinite. In an inhomogeneous layer the elements of the layer are coupled; the current distribution becomes defined. Electron or ion transport from neighboring elements influences via the balance of the charge carriers the voltage of an element. This effect can be taken care of by adding to the voltage $U_r(j)$ a diffusive term proportional to $-\Delta_\parallel j$. With these contributions the voltage balance of the layer gives the voltage across the inductance

$$l\frac{\partial j}{\partial t}=U_L-[U_r(j)-\gamma\Delta_\parallel j]\ , \tag{4}$$

where U_L is the total voltage across the layer, $U_r(j)$ is the voltage due to the nonlinear resistance, $\gamma\Delta_\parallel j$ is the voltage due to diffusive coupling; $\Delta_\parallel$ is the component of the Laplacian parallel to the electrode, γ is the coefficient of diffusive coupling of neighboring elements of the layer, and l is the inductance of an unit area, taking into account relaxation effects. This equation represents a Ginsburg-Landau equation or a reaction-diffusion equation; effects of relaxation and diffusion are taken into account by linear terms. At the border line $\mathbf{r}=\mathbf{r}_b$ of the electrode the current density disappears,

$$j=0 \quad \text{for } \mathbf{r}=\mathbf{r}_b\ . \tag{5a}$$

In some cases a free boundary of a spot exists,

$$j=0 \quad \text{for } \nabla_{\parallel n} j=0\ , \tag{5b}$$

where $\nabla_{\parallel n}$ describes the component of the gradient parallel to the surface and normal to the free boundary of the spot. The layer equation (4) can be normalized

$$\frac{\partial\tilde{j}}{\partial\tilde{t}}=\tilde{U}_L-(\tilde{U}_r(\tilde{j})-\tilde{\Delta}_\parallel\tilde{j}) \tag{6}$$

using the dimensionless variables

$$\tilde{j}=\frac{j}{j_{sc}}\ , \tag{7a}$$

$$\tilde{U}=\frac{U}{U_{sc}}\ , \tag{7b}$$

$$\tilde{t}=\frac{t}{\tau}\ , \tag{7c}$$

$$\tilde{\Delta}_\parallel=d^2\Delta_\parallel\ , \tag{7d}$$

the characteristic length

$$d=\left[\frac{\gamma j_{sc}}{U_{sc}}\right]^{1/2}\ , \tag{8}$$

TABLE II. Low and high current modes of different electrodic layers.

Discharge parts \ Model zones	Low current mode	High current mode	Bistable characteristic (Reference
Cathodic layer of the glow discharge	non-ignited mode	cathodic parts of the glow discharge	Hantzsche (Ref. 14)
Anodic layer of the glow discharge	anode glow	anode spots	Rubens and Henderson (Ref. 5)
Cathodic layer of the arc	cathodic parts of the glow discharge	cathode spot of the arc	Finkelnburg and Maecker (Ref. 15)

the characteristic time

$$\tau=\frac{lj_{sc}}{U_{sc}}\ , \tag{9}$$

and the scaling quantities U_{sc}, j_{sc} to be taken from the $U_r(j)$ characteristic. From the current density j through the layer the total current can be calculated by integration over the total area A of the electrode,

$$I=\int_A dA\, j\ . \tag{10}$$

C. Variational description

The right-hand side of Eq. (4) shall be reformulated into a variational description. The current density j is taken as independent variable; the variation is performed at a fixed time t and with the boundary condition (5). Contributions of the layer and the external circuit to a generalized potential F are introduced,

$$F_E=-U_B I+\tfrac{1}{2}R_E I^2\ , \tag{11}$$

$$F_L=\int_A dA\left[\int_0^j U_r(\bar{j})d\bar{j}+\tfrac{1}{2}\gamma(\nabla_\parallel j)^2\right]\ . \tag{12}$$

The corresponding variational derivatives are

$$\frac{\delta F_E}{\delta j}=-U_B+R_E I\ , \tag{13}$$

$$\frac{\delta F_L}{\delta j}=U_r(j)-\gamma\Delta_\parallel j\ , \tag{14}$$

using Eq. (10). The equation of motion of the layer, Eq. (4), can be written as

$$l\frac{\partial j}{\partial t}=-\frac{\delta F}{\delta j}\ , \tag{15}$$

with a generalized potential,

$$F=F_E+F_L\ . \tag{16}$$

During relaxation of the distribution j towards a steady state, the value of F decreases,

$$\frac{dF}{dt}\le 0 \tag{17}$$

until a minimum,

$$\delta F=0\ , \tag{18}$$

i.e., a stable (or metastable) steady state ($d/dt=0$) is reached. In the neighborhood of this state the condition

$$\delta F>0 \tag{19}$$

holds. Thus F represents a Lyapunov functional of the differential equation (4). A local minimum represents a metastable state, a global minimum a stable state.

A layer obeying Eq. (15) is governed by the principle of minimum F. Analogous situations in gas discharges have been discussed by the author recently.[18] According to Glansdorff and Prigogine,[19] the increment δF, derived from Eqs. (11), (12), and (16), in the neighborhood of a steady state may be termed "excess energy dissipation." The gradient term in F provides steady states with smooth density distributions $j(\mathbf{r})$, analogously to the surface energy of a droplet.

D. Steady spotlike profiles

Steady spotlike profiles $j(\rho)$ of radial symmetry located on a plane electrode shall be investigated. Here the normalized layer equation (6) can be reduced to

$$\frac{d^2j}{d\rho^2}=-\frac{1}{\rho}\frac{dj}{d\rho}-[U-U_r(j)]=-\frac{1}{\rho}\frac{dj}{d\rho}-\frac{dV}{d\rho}\ , \tag{20}$$

ρ being the radial coordinate and U the voltage of the steady spot. The wavy lines, indicating the normalization of the variables, Eq. (7), have been omitted; the potential

$$V(j)=\int_0^j[U-U_r(\bar{j})]d\bar{j} \tag{21}$$

is introduced. At the border of the electrode, Eq. (5a) shall be fulfilled. Equation (20) is analogous to the (normalized) equation of motion of a particle under the influence of a force of potential $V(x)$ and a time dependent damping term

$$\frac{d^2x}{dt^2}=-\frac{1}{t}\frac{dx}{dt}-\frac{dV}{dx}\ . \tag{22}$$

With the help of this analogy the formation of a spot can be discussed qualitatively; the S-shaped characteristic $U_r(j)$ of Fig. 2 shall be used. The lower diagram of Fig. 4(a) shows a small spot located on the background of constant current density j_l; at the boundary of the electrode the current density goes to zero. In the particle picture of Fig. 4(a) the particle starts from the position indicated by a dot. Due to the initial damping it just reaches the left maximum at $x=x_l$, coming practically to rest there; eventually it continues its course to $x=0$. In Fig. 4(b) a

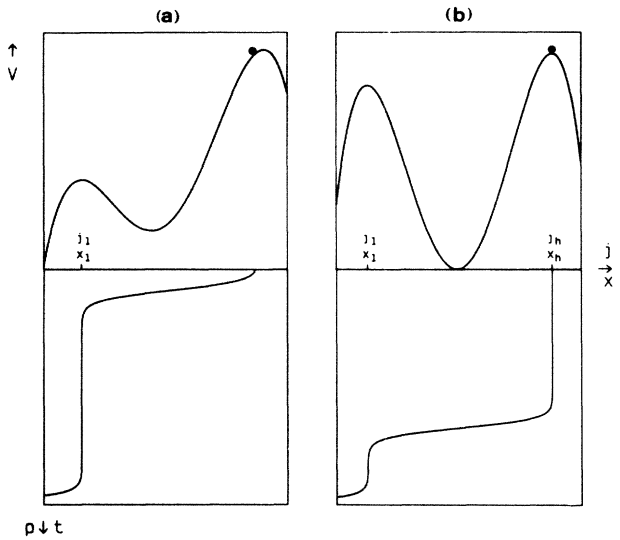

FIG. 4. Potential distribution $V(j)$ or $V(x)$ (upper part) and radial density profile $j(\rho)$ or motion of particle $x(t)$ (lower part). (a) $U_L/U_{crit}=1.15$, small spot; (b) $U_L/U_{crit}=1.02$, large spot.

large spot with the density j_h in the center on the background of the density j_l is shown. For a very large spot of density j_h on a very large background of density j_l, i.e., in the asymptotic case, the two maxima of V at $j=j_l,j_h$ are equal:

$$V(j_h)-V(j_l)=\int_{j_l}^{j_h}[U-U_r(\bar{j})]d\bar{j}=0\ , \tag{23}$$

$$\frac{dV}{dj}=U-U_r(j)=0 \quad \text{for } j=j_l,j_h\ . \tag{24}$$

This leads to Maxwell's construction, originally applied to van der Waals's relation for a real gas (see, e.g., Huang[20]),

$$U=U_{\text{crit}}\ , \tag{25}$$

in Fig. 2. Here two homogeneous phases j_l and j_h exist.

Due to the discussion above it becomes evident that the existence of two phases is coupled with the existence of an S-shaped $U_r(j)$ characteristic of the layer. The separation of the phases and thus spot formation is caused by the gradient term in F_L of Eq. (12) analogous to a surface energy.

Integration of Eq. (20) leads to a voltage-current characteristic $U(I)$ of a spot. As indicated by the examples of Fig. 4, the spot voltage U decreases with increasing spot current I, and the differential resistance dU/dI is negative and vanishes in the asymptotic case $I\to\infty$.

For a special shape of $U_r(j)$, the current density j_l of the background may be negligible ("dark" background); a free boundary exists [Eq. (5b)], a definite radius of a spot can be given. Steady solutions of Eq. (20) may be built up by superimposing the individual profiles of N spots not overlapping each other and each possessing the same voltage and thus the same currents and radii.

E. Quasisteady spots, equations of motion

A system of spots close to a steady state shall be investigated. Each spot α located with its center at $\mathbf{r}_\alpha$, is assumed to possess a quasisteady profile j_s, calculated from Eq. (20) for the instantaneous value of the spot current $I_\alpha(t)$. If a current density j_l of the background is negligible, the density distribution $j(\mathbf{r},t)$ of the system can be constructed by a superposition

$$j(\mathbf{r},t)=\sum_{\alpha=1}^{N} j_s(\,|\,\mathbf{r}-\mathbf{r}_\alpha(t)\,|\,,I_\alpha(t)) \tag{26}$$

with the total current

$$I=\sum_{\alpha=1}^{N} I_\alpha=\sum_{\alpha=1}^{N}\int_{A_\alpha} dA\, j\ , \tag{27}$$

where each integral is extended over the electrodic area A_α of the corresponding spot α.

To find an equation of motion of the spots, governing the parameters $I_\alpha(t)$ and $\mathbf{r}_\alpha(t)$, one enters with the distribution (26) into the integrated and equivalent version of Eq. (15),

$$\int_A dA\, l\frac{\partial j}{\partial t}\delta j=-\delta F\ . \tag{28}$$

This method is not unique; before integration Eq. (15) may be multiplied by an arbitrary function $f(j)$. However, since Eq. (28) represents a power balance, $f(j)$ is set equal to 1. Using Eqs. (13), (14), (26) and (27), the contributions to Eq. (28) can be written as

$$\int_A dA\, l\frac{\partial j}{\partial t}\delta j=\sum_{\alpha=1}^{N}\left[L(I_\alpha)\frac{dI_\alpha}{dt}\delta I_\alpha+M_\alpha(I_\alpha)\frac{d\mathbf{r}_\alpha}{dt}\delta\mathbf{r}_\alpha\right], \tag{29}$$

$$-\int_A dA\frac{\delta F_L}{\delta j}\delta j=-\sum_{\alpha=1}^{N}U(I_\alpha)\delta I_\alpha =-\delta\left[\sum_{\alpha=1}^{N}\int_0^{I_\alpha}U(\bar{I}_\alpha)d\bar{I}_\alpha\right], \tag{30}$$

$$-\int_A dA\frac{\delta F_E}{\delta j}\delta j=(U_B-R_EI)\sum_{\alpha=1}^{N}\delta I_\alpha =-\delta(-U_BI+\tfrac{1}{2}R_EI^2)=-\delta F_E\ , \tag{31}$$

with the inductance of a quasisteady spot

$$L(I_\alpha)=2\pi l\int_0^\infty\left[\frac{\partial j_s(\rho,I_\alpha)}{\partial I_\alpha}\right]^2\rho\,d\rho \tag{32}$$

and its frictional coefficient

$$M(I_\alpha)=2\pi l\int_0^\infty\left[\frac{\partial j_s(\rho,I_\alpha)}{\partial\rho}\right]^2\rho\,d\rho\ . \tag{33}$$

The equations of motion result,

$$L(I_\alpha)\frac{dI_\alpha}{dt}=-\frac{\partial F}{\partial I_\alpha}=U_L-U(I_\alpha)\ , \tag{34}$$

$$M(I_\alpha)\frac{d\mathbf{r}_\alpha}{dt}=-\frac{\partial F}{\partial\mathbf{r}_\alpha}=0\ , \tag{35}$$

if (U_B-R_EI) is replaced by the layer voltage U_L. For the assumption of quasisteady spots, Eq. (26), the generalized potential

$$F=-U_BI+\tfrac{1}{2}R_EI^2+\sum_{\alpha=1}^{N}\int_0^{I_\alpha}U(\bar{I}_\alpha)d\bar{I}_\alpha \tag{36}$$

exists, being a Lyapunov function of the differential equations (34) and (35). The generalized forces $-\partial F/\partial I_\alpha$ or voltage overshoots $[U_L-U(I_\alpha)]$ change the currents I_α; the generalized forces $-\partial F/\partial\mathbf{r}_\alpha$, acting on the positions of the spot, vanish. Thus the spots show fixed positions $\mathbf{r}_\alpha$, given by the initial conditions. By the assumptions of quasisteady spots each spot is replaced by a nonlinear resistor voltage $U(I_\alpha)$ with negative differential resistance, $dU(I_\alpha)/dI_\alpha$ in series with an inductance $L(I_\alpha)$.

F. Quasisteady spots, stability analysis

The equations of motion (34) allow a stability analysis. From condition (19) or

$$\delta^2F=\sum_{\alpha,\beta=1}^{N}\frac{\partial^2F}{\partial I_\alpha\partial I_\beta}\delta I_\alpha\delta I_\beta>0\ , \tag{37}$$

with

$$\frac{\partial^2 F}{\partial I_\alpha \partial I_\beta} = R_E + \delta_{\alpha\beta}\frac{dU(I_\alpha)}{dI_\alpha}\,, \qquad \delta_{\alpha\beta} = \begin{cases} 0 & \text{for } \alpha \neq \beta \\ 1 & \text{for } \alpha = \beta\,, \end{cases} \tag{38}$$

the stability criterion

$$\begin{vmatrix} \frac{\partial^2 F}{\partial I_1 \partial I_1} & \cdots & \frac{\partial^2 F}{\partial I_1 \partial I_\alpha} \\ \vdots & & \vdots \\ \frac{\partial^2 F}{\partial I_\alpha \partial I_1} & \cdots & \frac{\partial^2 F}{\partial I_\alpha \partial I_\alpha} \end{vmatrix} > 0, \quad 1 \le \alpha \le N \tag{39}$$

for a steady state can be derived (see, e.g., Salle and Lefshetz[21]). Evaluation leads to

$$\left[1 + R_E \sum_{\beta=1}^{\alpha} \left[\frac{dU(I_\beta)}{dI_\beta}\right]^{-1}\right] \prod_{\beta=1}^{\alpha} \frac{dU(I_\beta)}{dI_\beta} > 0\,, \qquad 1 \le \alpha \le N\,. \tag{40}$$

Because of the negative differential resistance $dU(I)/dI$ of a spot, one single spot may be stabilized by an external resistor

$$R_E + \frac{dU(I)}{dI} > 0\,. \tag{41}$$

A pattern of several identical spots is unstable and changes to a single large spot. For perturbations obeying the assumption (26) of quasisteady spots, only one spot is stable.

G. Application to the normal glow discharge

The normal glow discharge only partly covering the cathode can be interpreted as a spot with a free boundary [Eq. (5b)] on a black background ($j_l = 0$). Maxwell's construction [Eqs. (23) and (24), see Fig. 2] determines the voltage U_{crit} for a large spot, i.e., the normal cathode fall. The resulting value depends on the shape of the $U_r(j)$ characteristic and exceeds the minimum value $U_{\min}$. While $U = U_{\text{crit}}$ leads to a distribution $j(\rho)$, which drops to zero at the free boundary, $U = U_{\min}$ produces a homogeneous distribution without boundary. Rothhard[22] has investigated this problem experimentally. The homogeneous distribution was realized by a surrounding auxiliary discharge. A difference of a few volts between the normal cathode fall and the minimum cathode fall was found.

III. LAYER IN CONTACT WITH A RESISTIVE REGION, PATTERN OF SPOTS

A. Model

In this section the interelectrodic space shall consist of a thin electrodic layer, obeying Eqs. (4) and (5), and a resistive region of constant conductivity σ. Due to the voltage drop $U_{RR}(\mathbf{r}_L)$ across the resistive region the layer voltage $U_L(\mathbf{r}_L)$ depends on the position $\mathbf{r}_L$ at the layer [see Eq. (1)].

The current transport through the layer shall be concentrated in spots where the layer is conducting. Outside of the spots the current density shall be negligible, the layer insulating.

At a nonsteady pattern of spots relaxing to a steady state the following interdependent processes may be observed.

Relaxation of the profiles of the spots.
Relaxation of the number of the spots, connected with birth and death of spots.
Relaxation of the currents I_α of the spots.
Relaxation of the pattern of spots.

In the following a pattern of N spots at an electrode, chosen to be the anode, shall be investigated on a time scale, where the first two processes are very fast.

To take into account the electrodic plasma of a spot, found experimentally, the contact of the layer to the resistive region at the spot is modeled by an ideally conducting volume on top of the spot acting as an interface. The (time-dependent) shape of this volume will be discussed in Sec. III C. The resistive region can be described by its electric potential φ obeying

$$\Delta\varphi = 0\,, \tag{42}$$

with the boundary conditions

$$I = -\sigma \int_{A_c} dA\, \nabla_n \varphi \tag{43}$$

at the cathode,

$$I_\alpha = \int_{A_{A\alpha}} dA\, j = \sigma \int_{A_{L\alpha}} dA\, \nabla_n \varphi \tag{44}$$

at a spot α,

$$\nabla_n \varphi = 0 \tag{45}$$

at the layer outside of the spots and at insulating walls, contacting the resistive region. The area $A_{A\alpha}$ refers to the part of the anode covered by the spot α, the area $A_{L\alpha}$ to the boundary of the resistive region to the interfacing volume on top of the spot α (see Fig. 5).

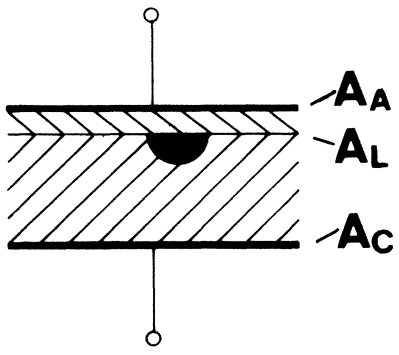

FIG. 5. Gas discharge model. ——: electrode; ▒▒: anodic layer; ▬: ideally conducting volume on top of a spot, interfacial volume; ▨: resistive region; A_A: boundary of the anode towards the layer; A_L: boundary of the resistive region towards the layer; A_C: boundary of the cathode towards the resistive region.

B. Variational description of the resistive region

In this section the description of the resistive region shall be fitted into the variational description of the layer of Sec. II with j as an independent variable. For a nonvanishing voltage drop $U_{RR}(\mathbf{r}_L)$ across the resistive region, Eq. (15) has to be replaced by

$$l\frac{\partial j}{\partial t}=-\frac{\delta(F_E+F_L)}{\delta j}-U_{RR}(\mathbf{r}_L)\ . \tag{46}$$

Here the last term to be transformed. From the variation of the functional

$$F^*_{RR}=\tfrac{1}{2}\sigma\int_{V_{RR}}dV(\nabla\varphi)^2\ , \tag{47}$$

which represents one half of the energy dissipation of the resistive region, one finds

$$\begin{aligned}\delta F^*_{RR}&=\tfrac{1}{2}\sigma\delta\int_{V_{RR}}dV(\nabla\varphi)^2\\&=-\sigma\int_{V_{RR}}dV\,\varphi\Delta\delta\varphi+\sigma\int_{A_L+A_C}dA\,\varphi\nabla_n\delta\varphi+\tfrac{1}{2}\sigma\int_{A_L}dA(\nabla\varphi)^2\delta s_n\\&=\int_{A_A}dA[\varphi(\mathbf{r}_L)-\varphi_C]\delta j+\tfrac{1}{2}\sigma\int_{A_L}dA(\nabla\varphi)^2\delta s_n=\int_{A_A}dA\,U_{RR}(\mathbf{r}_L)\delta j+\tfrac{1}{2}\sigma\int_{A_L}dA(\nabla\varphi)^2\delta s_n\end{aligned} \tag{48}$$

using Eqs. (10) and (42)–(45). The integral over A_L in the last line of Eq. (48) is caused by the change of the surface A_L, i.e., by the "breathing" of the spots during change of the current; a variation δj lets the interfacial volumes expand by a step δs_n in normal direction. The integrated version of Eq. (46) reads

$$\begin{aligned}\int_{A_A}dA\,l\frac{\partial j}{\partial t}\delta j=&-\delta(F_E+F_L+F^*_{RR})\\&+\tfrac{1}{2}\sigma\int_{A_L}dA(\nabla\varphi)^2\delta s_n\ .\end{aligned} \tag{49}$$

Due to the breathing of the spots no Lyapunov functional can be given.

C. Small quasisteady spots, motion and stability

The assumption of quasisteady spots, Eq. (26), shall be connected with the assumption of a hemispherical shape (radius ρ_α) of the interfacial volume on top of each spot. Using these assumptions Eq. (49) leads to the equations of motion

$$\begin{aligned}L(I_\alpha)\frac{dI_\alpha}{dt}=&-\frac{\partial(F_E+F_L+F^*_{RR})}{\partial I_\alpha}\\&+\tfrac{1}{2}\sigma\frac{d\rho_\alpha}{dI_\alpha}\int_{A_{L\alpha}}dA(\nabla\varphi)^2\\=&\,U_D-U_{RR\alpha}-U(I_\alpha)=U_{L\alpha}-U(I_\alpha)\ ,\end{aligned} \tag{50}$$

$$M(I_\alpha)\frac{d\mathbf{r}_\alpha}{dt}=-\frac{\partial F^*_{RR}}{\partial\mathbf{r}_\alpha}\ . \tag{51}$$

The energy dissipation of a resistive region, bounded by N ideal conductors of area $A_{L\alpha}$, by the cathode, by the insulating parts of the anode, and some insulating walls can be expressed as a bilinear form in the currents I_α:

$$F^*_{RR}=\tfrac{1}{2}\sum_{\alpha,\beta=1}^{N}R_{\alpha\beta}I_\alpha I_\beta \tag{52}$$

with the coefficients of resistivity

$$R_{\alpha\beta}(I_1,\ldots,I_N,\mathbf{r}_1,\ldots,\mathbf{r}_N)\ .$$

Reference to the electrostatic analogy (Table III) may help to evaluate the coefficient $R_{\alpha\beta}$.

For small spots

$$\rho_\alpha\ll|\mathbf{r}_\alpha-\mathbf{r}_\beta|\ ,\quad\beta\neq\alpha \tag{53}$$

and a distant cathode, nearly the total voltage

$$U_{RR\alpha}=\sum_{\beta=1}^{N}R_{\alpha\beta}I_\beta \tag{54}$$

drops in the close neighborhood of the spot α, practically independently of the currents I_β ($\beta\neq\alpha$), of the other spots. Thus for the relaxation of the spot currents I_α [Eq. (50)] the voltage $U_{RR\alpha}$ can be replaced by

$$U_{RR\alpha}=R_{\alpha\alpha}I_\alpha=\frac{\partial}{\partial I_\alpha}\int_0^{I_\alpha}R_{\alpha\alpha}(\bar{I}_\alpha)d\bar{I}_\alpha\ . \tag{55}$$

With the new function

$$F_{RR}=\sum_{\alpha=1}^{N}\int_0^{I_\alpha}R(\bar{I}_\alpha)d\bar{I}_\alpha,\quad R(I_\alpha)\equiv R_{\alpha\alpha}(I_\alpha) \tag{56}$$

one finds the final form of the first equations of motion,

$$L(I_\alpha)\frac{dI_\alpha}{dt}=-\frac{\partial(F_E+F_L+F_{RR})}{\partial I_\alpha}\ . \tag{57}$$

Due to the approximation (55) the relaxation of the currents, Eq. (57), is decoupled from the relaxation of the positions, Eq. (51). In a first phase the currents relax, governed by a Lyapunov function

$$F=F_E+F_L+F_{RR}\ . \tag{58}$$

Since F_{RR} is symmetric in the currents I_α, in a steady state all spots possess the same currents. In a second phase on a larger time scale the positions relax, governed by the Lyapunov function

$$F^*=F^*_R\ . \tag{59}$$

Here the interaction terms, neglected in approximation

TABLE III. Analogy of the current density field with the electrostatic field.

Resistive region of conductivity σ	Dielectric region of permittivity ϵ
Electric potential φ	Electric potential φ
N ideally conducting volumes of hemispherical shape in front of the spots	N hemispherical conductors
Cathode, reference electrode	Reference conductor
Boundaries to insulating material ($\sigma=0$) representing the nonconducting parts of the layer and insulating walls	Boundary to material with $\epsilon=0$
Current I_α to the spot α	Charge Q_α of the conductor α
$0.5\times$ energy dissipation: $\frac{1}{2}\sigma\int(\nabla\varphi)^2dV=\frac{1}{2}\sum_{\alpha,\beta=1}^{N}R_{\alpha\beta}I_\alpha I_\beta$	Electrostatic energy (see e.g. Jeans [Ref. 23]): $\frac{1}{2}\epsilon\int(\nabla\varphi)^2dV=\frac{1}{2}\sum_{\alpha,\beta=1}^{N}P_{\alpha\beta}Q_\alpha Q_\beta$
Coefficient $R_{\alpha\beta}$ of resistivity ($R_{\alpha\beta}=R_{\beta\alpha}$)	Coefficient $P_{\alpha\beta}$ of potential
Voltage $U_{RR\alpha}$ between the conductor α and the cathode $U_{RR\alpha}=\sum_{\beta=1}^{N}R_{\alpha\beta}I_\beta$	Voltage U_α between the conductor and the reference conductor $U_\alpha=\sum_{\beta=1}^{N}P_{\alpha\beta}Q_\beta$

(55), are important.

Now the stability of a pattern of spots is analyzed with respect to a perturbation δI_α analogously to Sec. II F; in Eqs. (37)–(41) $U(I_\alpha)$ has to be replaced by the total voltage, sustaining a spot:

$$U_{\text{tot}}(I_\alpha)=U(I_\alpha)+R(I_\alpha)I_\alpha\ . \tag{60}$$

The stability criterion (40) leads for a single spot to

$$R_E+\frac{dU_{\text{tot}}(I)}{dI}>0\ . \tag{61}$$

The resistive region acts as a nonlinear series resistor R in front of the spot and helps to stabilize it. For a pattern of spots the criterion (40) asks for at least $(N-1)$ spots positive differential resistances

$$\frac{dU_{\text{tot}}(I_\alpha)}{dI_\alpha}>0\ . \tag{62}$$

Since in a steady state all spots possess the same current, for a pattern of spots condition (62) must hold for each spot. It can be shown that the global minimum for a pattern of many spots, $N\gg1$, can be constructed by Maxwell's construction applied to the characteristic $U(I)+R(I)I$.

D. Application to anode spots in a glow discharge

1. Plane anode

The electrostatic analogy of the spot system is constructed by starting with N positively charged spherical conductors, their centers located in a plane. The field is symmetric with respect to the plane; no field line crosses this plane. The electrostatic field at one side of this plane represents the electrostatic analogy of our spot system; its energy is given by

$$W=\frac{1}{2}\sum_{\alpha,\beta=1}^{N}P_{\alpha\beta}Q_\alpha Q_\beta\ , \tag{63}$$

Q_α being the charges of the hemispheres. The term $P_{\alpha\alpha}Q_\alpha^2/2$ represents the field energy if only one conductor α is charged. Neglecting for small conductors [condition (53)] the polarization of the other noncharged conductors one can write

$$\frac{1}{2}P_{\alpha\alpha}Q_\alpha^2=\frac{1}{2}\frac{2}{4\pi\epsilon\rho_\alpha}Q_\alpha^2\ , \tag{64}$$

where the factor 2 is due to the restriction to the half space. The term $P_{\alpha\beta}Q_\alpha Q_\beta$ gives the interaction energy of the two charges Q_α, Q_β, which for small conductors becomes

$$P_{\alpha\beta}Q_\alpha Q_\beta=\frac{2}{4\pi\epsilon\,|\,\mathbf{r}_\alpha-\mathbf{r}_\beta\,|}Q_\alpha Q_\beta\quad(\alpha\neq\beta)\ . \tag{65}$$

From Eqs. (64) and (65) the expressions for the analogous coefficients $R_{\alpha\beta}$ may be constructed.

Now the relaxation of a pattern of N spots is discussed. The currents I_α shall already be relaxed to the constant value I_s. The generalized potential F_{RR}^* of Eq. (52) reads

$$F_{RR}^*=I_s^2\sum_{\alpha=1}^{N}\sum_{\beta=1}^{\alpha-1}\frac{2}{4\pi\sigma\,|\,\mathbf{r}_\alpha-\mathbf{r}_\beta\,|}+\text{constant terms}\ . \tag{66}$$

The spots show a Coulomb-type of repulsive interaction. For a small number of spots all spots will move to the border. Berezin[24] investigated Coulombic interacting spots on a circular disc and calculated the configuration with the global minimum of energy. For $N \leq 11$ all spots were located at the border, for $N=12$ one spot in the center appeared. Problems occur at an experimental realization of the calculated situation; the anode has to be embedded into an insulating plane such that the current density field cannot extend behind the plane given by the surface of the anode.

2. *Hemispherical or spherical anode*

In this case no simple method exists to calculate $R_{\alpha\beta}$. For a spherical or hemispherical anode of radius r_A the Coulombic interaction terms in Eq. (66) shall be adapted approximating the distances $|\mathbf{r}_\alpha - \mathbf{r}_\beta|$ of the spots by their distances along the anode surface

$$r_{\alpha\beta} = r_A \arccos[\sin\vartheta_\alpha \sin\vartheta_\beta \cos(\varphi_\alpha - \varphi_\beta) + \cos\vartheta_\alpha \cos\vartheta_\beta] \ . \tag{67}$$

Here spherical coordinates $(\vartheta_\alpha, \varphi_\alpha)$ are introduced.

Up to now the influence of the cathode or of the grounded collector in the analogy has been neglected. This assumption is valid, e.g., as in the experiment of Rubens and Henderson,[5] if a spherical anode is surrounded by a large concentric cathode. Spots equally distributed over the anode are found. In our experiment, however (see Fig. 6), the influence of the cathode has to be taken into account; here the resistance $R_{\alpha\alpha}$ depends on the location of the spot on the anode and is smallest for $\vartheta_\alpha = 0$, the position closest to the cathode. Taking into account the prolonged path of the current from the spot to the cathode by an additional contribution to $R_{\alpha\alpha}$ being proportional to ϑ_α^n, the potential F^*_{RR} reads

$$F^*_{RR} = C_1 \sum_{\alpha=1}^{N} \sum_{\beta=1}^{\alpha=1} \frac{r_A}{r_{\alpha\beta}} + C_2 \sum_{\alpha=1}^{N} \vartheta_\alpha^n + \text{ const terms} \ , \tag{68}$$

with

$$C_1 \sim I_s^2 / [\sigma(I_s) r_A] \ , \tag{69a}$$

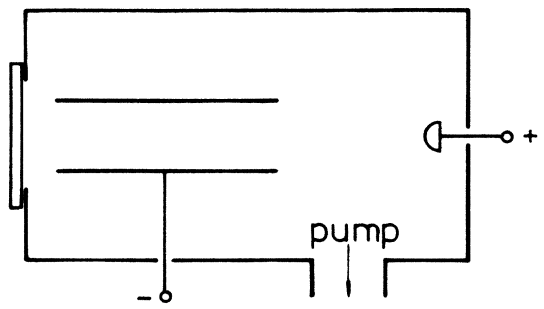

FIG. 6. Vacuum vessel with electrodic configuration; inner diameter and length of the cylindrical cathode: 4 cm and 12 cm; diameter of the hemispherical anode: 1.5 cm. The electrodic configuration is drawn in scale.

$$C_2 \sim I_s^2 r_A / \sigma(I_s) \ . \tag{69b}$$

The open parameters, namely the ratio C_1/C_2 and the exponent n, are assumed to be independent of the current and are fitted by comparison with the experiment; C_1 is set equal to 2. The resulting equations of motion read

$$\dot{\vartheta}_\alpha = -\frac{1}{M(I_s) r_A^2} \frac{\partial F^*_{RR}}{\partial \vartheta_\alpha} \ , \tag{70}$$

$$\dot{\varphi}_\alpha = -\frac{1}{M(I_s) r_A^2 \sin^2\vartheta_A} \frac{\partial F^*_{RR}}{\partial \varphi_\alpha} \ . \tag{71}$$

IV. ANODE SPOTS, EXPERIMENTS AND NUMERICAL CALCULATIONS

A. Experiments

Our experiments have been performed to produce patterns of spots in a glow discharge at a hemispherical anode. The experimental setup is sketched in Fig. 6. Within a metallic vessel a glow discharge in H_2 ($p=10$ mbar, $I=0.2$–1.0 A) was run between a cylindrical cathode and the anode. The vessel and electrodes consisted of steel. The anode was conditioned by cathodic operation. Symmetrical patterns of anode spots appeared (see Fig. 1), which were photographed through the window in front of the cathode. As a function of the discharge current the number of spots showed a pronounced hysteresis, whereas for a given number of spots on a freshly conditioned anode practically no geometrical hysteresis of the patterns was found. However, for certain spot numbers, two different patterns could be found, each occurring in a nonreproducible way in different runs of experiments. Visual appearance supports the assumption of approximately equal current I_s per spot in a given pattern. For the comparison with the calculated patterns situations with approximately constant current per spot were chosen.

B. Numerical calculation

The results of Sec. III D 2 are used. To find a steady pattern of N spots an initial pattern $(\vartheta_{\alpha 0}, \varphi_{\alpha 0})$ is assumed. Depending on the initial conditions different steady patterns with different values of F^*_{RR} may occur. For a calculated pattern the positions $(\vartheta_\alpha, \varphi_\alpha)$ of the centers of the spots are projected on a plane orthogonal to the axis of the electrodic configuration. In this projection each spot is marked by a full circle (see the right part of Fig. 1).

C. Discussion

The theoretically and experimentally found patterns agree surprisingly well. In most cases the patterns with minimum values of F^*_{RR}, i.e., the global minima, are realized. During other runs of the experiment some of the local minima and the global minima not realized in this experiment could be found. The success of these calculations support the basic ideas of the model, namely, the description of the discharge by an electrodic bistable layer and a resistive region.

The pattern of cathodic spots shown by Nechaev *et al.*[8] in a pulsed beam-driven discharge resemble those found at the anode of a glow discharge. Here our model of a bistable layer in contact with a resistive region should be applicable.

V. SUMMARIZING DISCUSSION

Formation of a single spot at the electrode of a gas discharge can be explained by a phenomenological model in which the electrodic phenomena are described by a bistable layer with an *S*-shaped voltage-current density characteristic. Patterns of spots occur if the bistable layer contacts a resistive medium, providing a series resistor for each spot and leading to a repulsive interaction of the spots. The model possesses a generalized potential or Lyapunov functional by which stable states as global minima and metastable states as local minima can be distinguished. Basic properties of electrodic plasma structures in gas discharges are explained. By adjusting two parameters of the model, patterns of anodic spots in glow discharges can be constructed in close agreement with the experimental ones. No efforts have been made to derive the parameters of the model equations, especially the voltage-current density characteristic, by starting from the elementary processes in the anodic region (see Emeleus[25]).

The calculation of anodic patterns may be compared with that of similar vortex patterns in a rotating superfluid (Campbell and Ziff[13]). The interaction of two anodic spots enters into the generalized potential F^*_{RR} by a three-dimensional Coulombic interaction term $1/|\mathbf{r}_\alpha-\mathbf{r}_\beta|$ [see Eq. (66)], whereas the interaction of two vortices produces a two-dimensional Coulombic term $\ln|\mathbf{r}_\alpha-\mathbf{r}_\beta|$ in the free energy of the vortex system. In addition the free energy contains terms of the repulsive interaction of the vortices with the image vortices due to the radial boundary of the superfluid. Corresponding terms in F^*_{RR} for the anode spots may occur if an insulating plate is brought close to the anode, and thus hinders the current transport from the spots to the cathode. Recent experiments on Coulombic interacting single ions in a rf trap show regular patterns similar to those of Fig. 1 (Diedrich, Peik, Chen, Quint, and Walther[26]).

ACKNOWLEDGMENT

I thank Mr. P. Mark for carrying out the numerical calculations and the experiments.

[1]G. Nicolis and I. Prigogine, *Self-Organization in Nonequilibrium Systems* (Wiley, New York 1977).

[2]H. Haken, *Synergetics* (Springer, Berlin 1978); *Advanced Synergetics* (Springer, Berlin 1983).

[3]*Self-Organization by Nonlinear Irreversible Processes,* edited by W. Ebeling and H. Ulbricht (Springer, Berlin, 1986).

[4]C. H. Thomas and O. S. Duffendack, Phys. Rev. **35**, 72 (1930).

[5]S. M. Rubens and J. E. Henderson, Phys. Rev. **58**, 446 (1940).

[6]R. E. Packard, Physica B **109&110**, 1474 (1982).

[7]I. G. Kesaev, Zh. Tekh. Fiz. **33**, 603 (1963) [Sov. Phys.—Tech. Phys. **8**, 447 (1963)].

[8]A. A. Nechaev, Yu. V. Orlov, I. G. Persiantsev, A. T. Rakhimov, and S. P. Rebrik, Fiz. Plazmy **12**, 441 (1988) [Sov. J. Plasma Phys. **12**, 255 (1986)].

[9]Ch. Radehaus, T. Dirksmeyer, H. Willebrand and H.-G. Purwins, Phys. Lett. A **125**, 92 (1987).

[10]K. G. Müller, in Proceedings of the Seventeenth International Conference on Phenomena in Ionized Gases, Budapest, 1985, p. 715 (unpublished).

[11]B. Ross and J. D. Litster, Phys. Rev. A **15**, 1246 (1977).

[12]R. Landauer, Phys. Rev. A **15**, 2117 (1977).

[13]L. J. Campbell and R. M. Ziff, Phys. Rev. B **20**, 1886 (1979).

[14]E. Hantzsche, Beitr. Plasmaphys. **1**, 203 (1961).

[15]W. Finkelnburg and H. Maecker, *Elektrische Bogen und Thermisches Plasma,* Vol. XXII of *Handbuch der Physik,* edited by J. S. Bakos and Zsuzsa Sörlei (Springer, Berlin, 1956), Sec. 263.

[16]A. L. Ward, J. Appl. Phys. **33**, 2789 (1962).

[17]V. N. Melekhin and N. Yu. Naumov, Pis'ma Zh. Tekh. Fiz. **12**, 99 (1986) [Sov. Tech. Phys. Lett. **12**, 41 (1986)].

[18]K. G. Müller, in *Proceedings of the Eighteenth International Conference on Phenomena in Ionized Gases, Swansea, 1987,* edited by W. Terry Williams (Hilger, Bristol, 1987), p. 186.

[19]P. Glansdorff and I. Prigogine, *Thermodynamic Theory of Structure, Stability and Fluctuations* (Wiley, London, 1971).

[20]K. Huang, *Statistische Mechanik I* (Bibliographisches Institut, Mannheim, 1964).

[21]J. La Salle and S. Lefschetz, *Die Stabilitätstheorie von Ljapunov* (Bibliographisches Institut, Mannheim, 1967), p. 38.

[22]L. Rothhardt, in *Proceedings of the Fifth International Conference on Ionization Phenomena in Gases, Munich, 1961* (North-Holland, Amsterdam, 1962), Vol. I, p. 290.

[23]J. Jeans, *The Mathematical Theory of Electricity and Magnetism* (Cambridge University Press, Cambridge, 1966), p. 93.

[24]A. A. Berezin, Chem. Phys. Lett. **123**, 62 (1986).

[25]K. G. Emeleus, Int. J. Electron. **52**, 407 (1982).

[26]F. Diedrich, E. Peik, J. M. Chen, W. Quint, and H. Walther, Phys. Rev. Lett. **59**, 2931 (1987).